

Mapping Low-Reflectance Material on Mercury

R. Klima (1), D. Blewett (1), B. Denevi (1), C. Ernst (1), S. Murchie (1), and P. Peplowski (1). (1) Johns Hopkins University Applied Physics Laboratory, Laurel, MD, USA. (Rachel.Klima@jhuapl.edu / Fax: +1-443-778-8939

Abstract

Distinctive low-reflectance material (LRM) was first observed on Mercury in Mariner 10 flyby images [1]. Visible to near-infrared reflectance spectra of LRM are flatter than the average reflectance spectrum of Mercury, which is strongly red sloped (increasing in reflectance with wavelength). From Mariner 10 and early Mercury, Surface, Space, ENvironment, GEochemistry, and Ranging (MESSENGER) flyby observations, it was suggested that a higher content of ilmenite, ulvöspinel, carbon, or iron metal could cause both the characteristic dark, flat spectrum of LRM and the globally low reflectance of Mercury [1,2]. Once MESSENGER entered orbit, low Fe and Ti abundances measured by the X-Ray and Gamma-Ray Spectrometers ruled out ilmenite and ulvöspinel as important surface constituents [3,4] and implied that LRM was darkened by a different phase, such as carbon or small amounts of micro- or nanophase iron or iron sulfide dispersed in a silicate matrix. Low-altitude thermal neutron measurements of three LRM-rich regions confirmed an enhancement of 1–3 wt% carbon over the global abundance, supporting the hypothesis that the darkening agent in LRM is carbon [5].

1. Distribution of LRM

LRM is distributed across Mercury, typically having been excavated from depth by craters and basins. In contrast to the brighter high reflectance plains (HRP) and smooth plains deposits, which exhibit morphological evidence of volcanism [e.g., 6-8], LRM is not associated with flow features or other evidence of a volcanic origin. Older LRM boundaries are generally diffuse, and grade into low-reflectance blue plains (LBP). Because of the common lack of sharp geologic boundaries, LRM has been defined primarily based on albedo and spectral shape, isolated through principal components (PC) analyses of MDIS color images [9]. LRM is the darkest material on Mercury, with an albedo of 4–5% at 560 nm, and it exhibits a spectral slope that is substantially less red (increases less in brightness with increasing wavelength) than the rest of Mercury. The low iron content of Mercury's surface results in

a lack of the spectral absorption bands typically used to map mafic minerals on planets and asteroids. Thus, mathematical transformations such as PC analysis are required to map subtle spectral differences. For example, the second principal component (PC2), captures a combination of spectral slope and curvature, isolating LRM and hollows as one endmember, with red material and HRP as the other end member. LBP and intermediate plains (IP) are transitional from LRM to HRP [10]. In [5], concentrated LRM exposures were defined as regions with a photometrically corrected reflectance of <5% (at 560 nm wavelength) and a PC2 value of <0.023. This value corresponds with the lower ~25% of the range of PC2 values for the whole planet. The resulting LRM map, overlain on the global color mosaic, is shown in Fig. 1a. There are some regional concentrations where many moderate sized craters or several larger basins excavated LRM in close proximity to one another. LRM is most immediately recognizable visually when excavated by craters and deposited onto high-reflectance red plains (HRP, as in Caloris basin), due to the contrasting reflectance and spectral slopes of the different stratigraphic layers. However, it is also abundant throughout the oldest, rough terrains, where its boundaries are more difficult to delineate as they grade into LBP. In these older terrains LRM is still apparently associated with crater ejecta, but the high density of craters excavating LRM results in a patchy distribution of low-reflectance, low-PC2 material.

2. Mapping LRM Directly

Because PC analyses are calculated using the spectral range over a given data set, a PC2 constraint cannot be directly translated to individual targeted color images, except in the rare case of images that contain the full range of Mercury's spectral diversity. The broad, shallow band centered near 600 nm that is observed in LRM (and also often in hollows material) can be isolated directly by dividing the planet as a whole by a reference spectrum and then calculating a band depth ratio. Murchie et al. [11] found that the most successful ratio for mapping the LRM was calculated by first dividing the full mosaic by a

reference spectrum of the northern volcanic plains, and then calculating the ratio as:

$$\sim 600 \text{ nm band depth} = 1 - \frac{(R_{560} + R_{630} + R_{750} + R_{830})/4}{(R_{900} + R_{480})/2}$$

where R is photometrically corrected reflectance in each of the given filters. Mapping this feature with the calibrated 8-color mosaic [12] clearly highlights the regions identified by the LRM map (Fig. 1b). However, isolating the LRM deposits also requires combining this band depth with an albedo constraint. We are currently developing a new ‘LRM’ parameter that captures the aspects of both the albedo and the spectral shape observed in the LRM and so far best parameterized by the 600 nm band depth calculation.

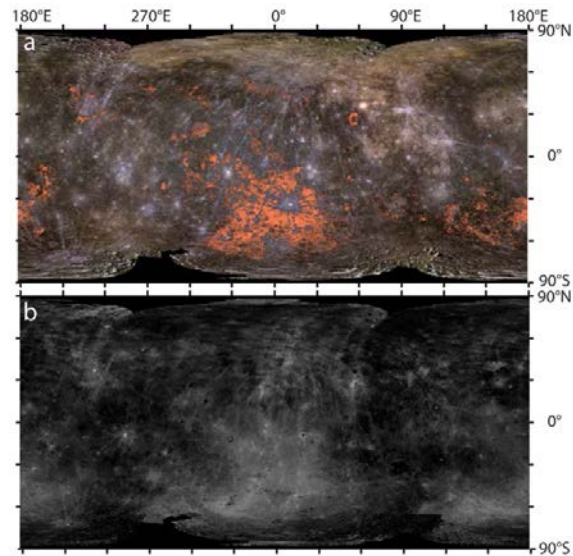


Fig. 1. (a) False color global map of Mercury with R=1000 nm, G=750 nm and B=430 nm. LRM shows up as dark bluish-black material, and grades into the slightly brighter LBP. The LRM map using albedo, PC2 and slope constraints as detailed in the text is overlaid in orange. (b) ~600-nm broad band depth map. From Klima et al., 2018.

3. Carbon Content of LRM

In [5], 600-nm band depth ratio in LRM was found to correlate with abundance of carbon as measured during low-altitude neutron detector measurements. Although there were only three locations that could be measured, within uncertainty, there is a clear linear relationship between the average ~600 nm band depth for each LRM deposit (mapped using the PC constraints previously described) and the measured carbon content. Based on the derived band-depth to carbon relationship, we estimated carbon

contents for other LRM deposits (Fig. 2). Our results suggest that some regions may contain as much as 5 wt% carbon above the global mean, a value consistent with the carbon content required to produce their low reflectances [11].

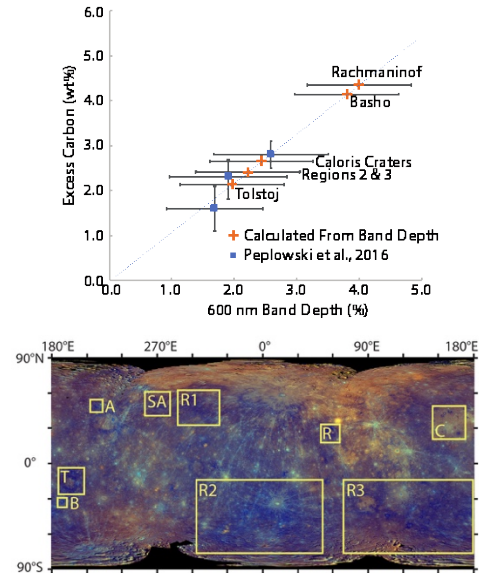


Fig. 2. (top) Extrapolated carbon content for different regions of the surface. Blue squares were measured directly in [5], orange pluses were calculated from the derived band depth relationship. (bottom) Enhanced color composite of Mercury with R=PC1, G=PC2, B=430/1000 nm slope. Locations of LRM-enriched craters measured in [5] A-Akutagawa, SA-Sholem-Aleichem, and R1-region LRM-A are shown, along with derived values for B-Basho, T-Tolstoj, R-Rachmaninoff and C-Craters within Caloris and two additional regional enhancements (R2, R3). From Klima et al., 2018.

Acknowledgements

We are grateful to the NASA PMDAP program for supporting this work (#NNX14AM93G).

References

- [1] Hapke, B. et al. (1975) *JGR* 80, 2431. [2] Robinson, M.S. et al. (2008) *Science* 321, 66. [3] Nittler, L.R. et al., (2011) *Science* 333, 1847. [4] Evans, R.G. et al. (2012) *JGR* 117, E00L07. [5] Peplowski, P.N. et al. (2016) *Nat. Geosci.* 9, 273-278. [6] Head, J.W. et al., (2011) *Science* 333, 1853-1856. [7] Whitten, J.L., et al. (2014) *Icarus* 241, 97-113. [8] Denevi, B.W. et al., (2013) *JGR Planets* 118, 891-907. [9] Klima, R.L., et al. (2016), *LPSC* 47, Abstract#1195. [10] Denevi, B. et al., (2016), *LPSC* 47, Abstract#1624. [11] Murchie, S.L. et al. (2015) *Icarus* 254, 287. [12] Denevi et al., (in press) DOI: 10.1007/s11214-017-0440-y. [13] Klima et al. [2018] *GRL*.